PHASE COMPOSITION, THERMAL BEHAVIOR AND MAGNETIC PROPERTIES OF ZINC- AND NICKEL-BEARING POWDERS FORMED ON THE STEEL SURFACE IN AN OPEN-AIR SYSTEM

O. Lavrynenko,[a]* N. Dudchenko,[b] O. Pavlenko[a] and A. Brik[b]

Keywords: Steel surface, nanoparticles, spinel ferrites, thermal transformation, superparamagnetics.

The nanosized powders formed on the steel surface in contact with aqueous solutions of zinc and nickel inorganic salts have been studied using an X-ray diffraction method, thermal analytical measurements (TG / DTG, DTA), scanning electron microscopy and magnetometry. It has been shown that a single mineral phase of a non-stoichiometric spinel ferrite is formed when zinc and nickel nitrate solutions were used as the dispersion medium, but in the presence of chloride-containing salts three mineral phases (spinel ferrite, lepidocrocite, and goethite) are formed in the phase composition of the surface powders. When sulfate solutions were chosen as the dispersion medium the mixed hydroxysulfate layered double hydroxides (LDHs) simultaneously appeared among other components of the powders. Due to cation exchange between Fe^{2+} and Zn^{2+} or Ni^{2+} the mixed LDH structures achieved stability against further oxidation and thermal transformation. Hence, the presence of mixed LDHs in the phase composition of the powders significantly complicates the obtaining of homogenous superparamagnetic 3*d*-metal doped spinel ferrite and iron oxide powders.

* Corresponding Author:
E-Mail: alena-lavry@yandex.ru
[a] Frantsevich Institute for Problems of Material Science of NAS of Ukraine, Kyiv, Ukraine
[b] M.P. Semenenko Institute of Geochemistry, Mineralogy and Ore Formation of NAS of Ukraine, Kiev, Ukraine

Introduction

Nowadays magnetic iron oxides – hematite, maghemite, and spinel ferrite (magnetite) have been recognized as a perspective material for biomedical applications.[1] So, gamma ferric oxide – maghemite, as a bio-comparable nanophase, is used for cell-separation, vector drug delivery, magnetic-induced hyperthermia, immune magnetic separation as well as it plays a role of a contrasting agent for the obtaining of the images applying magnetic resonance.[2-4] In addition, maghemite has unique magneto-optical[5] and catalytical[6] properties. Alpha ferric oxide – hematite possesses weak magnetic properties at Morin temperature (260 K)[7] and it is specified by complex ferromagnetic properties together with antiferromagnetic properties at *T* below 950 K.[8] Typically, hematite particles are used as a catalyst,[9] magnetic material,[10] pigment, inhibiting agent and reactant for soils remediation.[11]

Currently, the obtaining of 3*d*-metal doped iron oxide nanoparticles is carried out by various chemical and physical methods that include either gradual growth of primary precursor species (molecules or clusters) or dispergation of a bulk mineral phase or its microaggregates.[12] The small amount of transition 3*d*-metals in the structure of iron oxides may cardinally change their physical chemical properties and biological activity.[13] Hence, thermal homogenization of ferro- and ferrimagnetic disperse materials, varying magnetic properties of heated nanopowders and the presence or the absence of doped transition 3*d*-metal cations in a crystal lattice of iron oxides, in general, are widely discussed in the science sources.

The aim of the present work is to study the composition, thermal behaviour and magnetic properties of nickel- and zinc-bearing nanopowders formed on the steel surface in an open-air system.

Experimental

The rotating disk electrode made of steel 3 (St3), which has the composition (%): C 0.14-0.22, Si 0.05-0.15, Mn 0.4-0.5, Cr 0.3, Ni 0.3, P 0.04, S 0.05 and N 0.01, was chosen for obtaining of the raw iron-oxygen powders. The phase formation process was carried out in an open-air system under galvanostatic conditions via the rotation-corrosion dispergation route.[14] During the experiment, the electrode surface was alternately contacting with dispersion medium and air. Before every experiment the steel surface was exposed to mechanical treatment to remove an oxidized layer. Sulfuric acid was used for activating procedure. The activated steel electrode was repeatedly rinsed in water and onwards it was placed into the cell filled with distilled water or the 3*d*-metal water salt solution. Zinc and nickel chlorides, nitrates and sulfates were chosen to prepare the aqueous salt solution with the concentrations of cations as 100 mg dm^{-3} and pH of the solutions was set 6.5. The phase formation process was carried out in thermostat TS-1 /80-SPU and it lasted 24 h at 20 and 50 °C, afterwards the disk electrode was dried in air. The prepared powders were annealed in the induction furnace SNOL 6.7/1300 for 1 h at 440 and 740 °C.

The phase composition of iron-oxygen powders was determined by X-ray diffraction (XRD) method, thermal analytical measurements (TG / DTG, DTA) and scanning

electron microscopy (SEM). The phase composition of the nanopowders was conducted using computer-aided X-ray diffractometer (DRON – UM1) equipped with two Soller's slits and filtered radiation of cobalt anode CoK_α. The rate of the recording was set $1°\cdot min^{-1}$ and the interfacial Woolf-Bragg's angle was made up to 80 degrees. The primary particle size was calculated according to the standard Debye-Scherrer's formula. Thermogravimetric and differential thermal analysis (TG-DTA) of the powders was performed in the static air atmosphere by derivatograph Q-1500D (Hungary). The record was made using computer data registration. The parameters of the pattern recording were the following: the samples of 150 mg were heated at the rate 10 °C min^{-1} from 20 to 1000 °C, the sensitivity was 20 mg, TG – 500, DTG – 500 and DTA – 250. The samples were placed into a corundum crucible and covered by quartz beaker to create an equal temperature field. A scanning electron microscopy (SEM) using JOEL-6700 microscope equipped with an energy-dispersive and cathode-luminescence attachment to obtain EDS-spectra permitted to estimate the morphology of the surface structures. The weight ratio of iron to the second 3*d*-metal (nickel or zinc) in the samples was evaluated using an X-ray fluorescence spectroscopy (XRFS) carried out in the automatic spectrometer (ElvaX) equipped with a titanium anode. The magnetic properties of the raw and annealed powders were estimated via magnetometry performed with the help of a magnetometer equipped by Hall sensor.

Results

Preparation of the raw powders

The colloid-chemical mechanisms of the formation of magnetite (spinel ferrite) particles in the natural systems are determined by red-ox conditions in the system and depend on the quantity of dissolved ferrous aquahydroxo forms in the dispersion medium. Our kinetic study[15] of the phase formation processes on the steel electrode surface in contact with water dispersion medium and air showed the development of hydroxycarbonate Green Rust layer within 1-3 h and its oxidation into lepidocrocite γ-FeOOH within 3-5 h. At that, to compare the phase composition of the iron-oxygen structures formed on the refined and oxidized steel surface we proposed the following procedure: at first the prepared and activated disk electrode was placed in distilled water at T = 20 °C for 1, 3, and 5 h or at T = 50 °C for 1 h, afterwards the dispersion medium was replaced with zinc or nickel salt solutions. For the comparison we chosen the samples formed under initial contact of the steel surface with corresponding salt solutions.

Phase composition of the raw powders

The X-ray diffraction data of the nickel- and zinc-iron-oxygen-containing structures formed on the steel surface in contact with corresponding chloride solutions within 24 h at 20 and 50 °C are presented in figure 1. Also, when the zinc chloride and nickel chloride solutions were in contact with activated surface of the steel electrode at T = 20 °C, the obtained powders included three iron-oxygen mineral phases such as spinel ferrite (magnetite) (JCPDS file No 19-0629) and polymorphic ferric oxyhydroxides – lepidocrocite γ-FeOOH (JCPDS file No 08-0098) and goethite α-FeOOH (JCPDS file No 17-536). The trace peaks of the Green Rust I are seen on the XRD-patterns of both systems. In all cases the structures of the oxihydroxides and spinel ferrites coexist in the phase composition of the powders at T = 20 °C. But spinel ferrite phase got the predominant importance when the temperature was enhanced up to 50 °C, and under the following conditions both ferric oxyhydroxides were present in the patterns only as the admixtures. Thus, the temperature of the phase formation process strongly influenced not only the phase composition of the surface powders but their crystallinity degree as well. Whereas the powders obtained at T = 20 °C may be characterized as weak crystalline structures, the spinel ferrite particles formed in the mentioned systems at T = 50 °C were well crystallized.

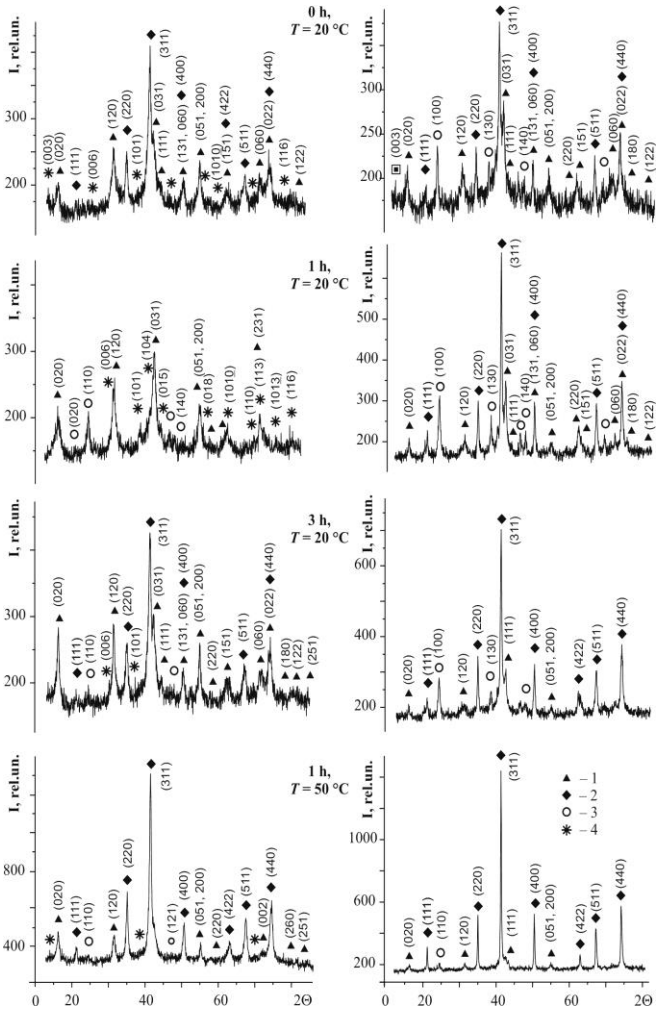

Figure 1. XRD-patterns of the powders formed on the steel surface contacting with the salt solutions: a – $ZnCl_2$; b – $NiCl_2$. Numbers correspond to the phases: 1 – lepidocrocite, 2 – spinel ferrite, 3 – goethite, 4 – Green Rust I.

When zinc and nickel sulfate solutions were chosen as the dispersion medium, the phase composition of the powders formed at T = 20 °C included mixed Zn(II)-Fe(II-III)-SO_4^{2-} and Ni(II)-Fe(II-III)-SO_4^{2-} layered double hydroxides (LDH) as a main mineral phase with an admixture of a relatively small amount of ferric oxihydroxides (Figure 2).

But when the *T* of the process was increased to 50 °C the mixed Ni(II)-Fe(II-III)-SO_4^{2-} LDH as well as spinel ferrite were determined as two main phases in the powders, but goethite and lepidocrocite played the role of mineral admixtures.

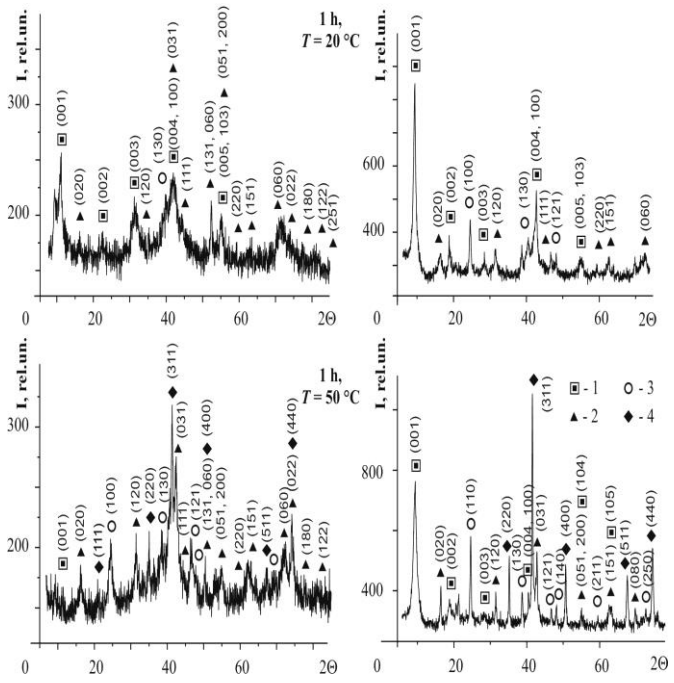

Figure 2. XRD-patterns of the powders formed on the steel surface contacting with the salt solutions: a – $ZnSO_4$; b – $NiSO_4$. Numbers correspond to the phases: 1 – Green Rust II, 2 – lepidocrocite, 3 – goethite, 4 – spinel ferrite.

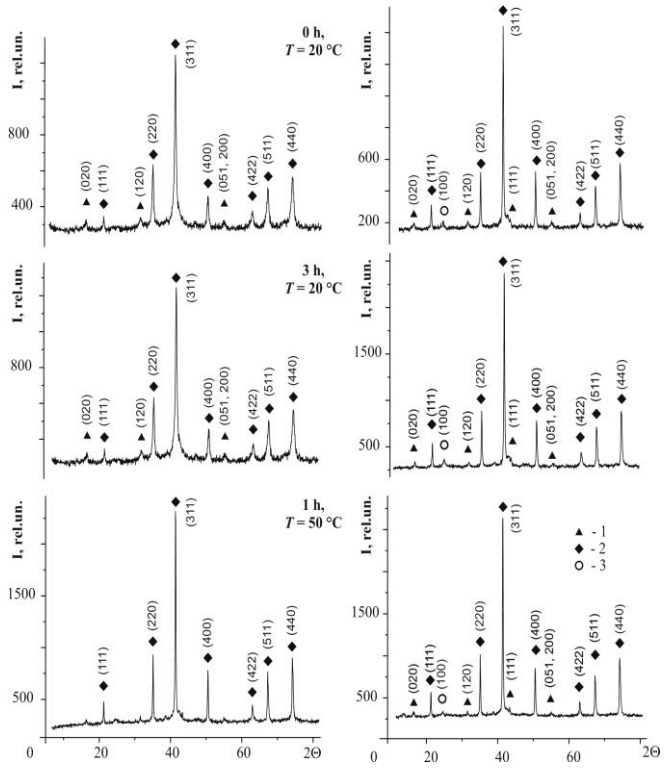

Figure 3. XRD-patterns of the powders formed on the steel surface contacting with the salt solutions: a – $Zn(NO_3)_2$; b – $Ni(NO_3)_2$. Numbers correspond to the phases: 1 – lepidocrocite, 2 – spinel ferrite, 3 – goethite.

But high-disperse weak crystalline phases of lepidocrocite and spinel ferrite phases coexist in zinc-bearing powders. According to the lattice parameters, the mixed LDH corresponds to hydrohonessite-like hydroxysulfate Green Rust II (JCPDS file No 41-0014). The usage of zinc and nickel nitrate solutions results in the formation of the homogeneous spinel ferrite phases at all temperature conditions (Figure 3). But the contact of high disperses spinel ferrites with air-oxygen results in the appearance of the small amount of ferric oxyhydroxides in the phase compositions of the powders. While the trace lepidocrocite peaks are clearly seen on the patterns of both systems, goethite is present only in the nickel-bearing powders.

Table 1. The lattice parameters (*a, b, c*) and primary particle size (*d*) of the powder components obtained on the steel surface

Salt solution	T, C°	The parameters of the mineral phases, nm		
		γ-FeOOH	α-FeOOH	Fe_3O_4
$NiCl_2$	20	*a*=0.3875	*a*=0.4649	*a*=0.8404
		b=1.2695	*b*=0.9946	*d*=21.9
		c=0.3022	*c*=0.3027	
		d=10.4	*d*=14.5	
	50	*a*=0.3875	*a*=0.4668	*a*=0.8419
		b=1.2630	*b*=0.9874	*d*=28.2
		c=0.2922	*c*=0.3007	
		d=13.3	*d*=21.0	
$NiSO_4$	20	*a*=0.3876	*a*=0.4630	*a*=0.8370
		b=1.2546	*b*=0.9969	*d*=24.8
		c=0.3059	*c*=0.3016	
		d=13.7	*d*=14.6	
	50	*a*=0.3889	*a*=0.4623	*a*=0.8389
		b=1.2608	*b*=0.9868	*d*=26,3
		c=0.3022	*c*=0.3001	
		d=20.0	*d*=18.9	
$Ni(NO_3)_2$	20	*a*=0.3872	*a*=0.4637	*a*=0.8386
		b=1.2599	*b*=0.9650	*d*=21.9
		c=0.3029	*c*=0.3022	
			d=23.2	
	50	–	–	*a*=0.8399
				d=26,3
$ZnCl_2$	20	*a*=0.3894	–	*a*=0.8399
		b=1.2527		*d*=9.9
		c=0.3079		
		d=8.9		
	50	*a*=0.3876	–	*a*=0.8395
		b=1.2638		*d*=10.4
		c=0.3067		
		d=13.3		
$ZnSO_4$	20	*a*=0.3858	*a*=0.4626	*a*=0.8404
		b=1.2692	*b*=1.0106	*d*=19.1
		c=0.3062	*c*=0.3013	
		d=21.7	*d*=16.2	
	50	*a*=0.3855	*a*=0.4636	*a*=0.8397
		b=1.2630	*b*=0.9950	*d*=27.4
		c=0.3044	*c*=0.3007	
		d=23.4	*d*=20.1	
$Zn(NO_3)_2$	20	–	–	*a*=0.8403
				d=15.8
	50	–	–	*a*=0.8398
				d=28.2

The crystal lattice parameters and the primary particle size (CSR) of the powder compounds are presented in table 1. As it is clearly seen, the CSR of lepidocrocite varies from ~10 to ~23 nm and the smallest particles correspond to chloride systems whereas the biggest particles relate to sulfate systems. The range of the goethite particle size is narrow in comparison with the previous case and it ranges from 14 to 23 nm. But variation of the magnetite CSR is more significant and we can see the smallest particles in zinc chloride systems (~10 nm). Generally, the average particle size of magnetite formed in nickel-containing systems is bigger than in zinc-containing systems and it is 22–28 nm in the first case and ~15–28 nm in the second case. The wt.% distribution of the metals in the powders formed in the presence of nickel- and zinc-containing water salt solutions is seen in table 2. Also, the weight ratio of iron to zinc is the most stable in zinc nitrate solutions and it gets 78 (82) : 22 (18) wt.%, but in the chloride-containing solution such parameter varies from 94 to 79 wt.%. (Fe) and from 6 to 21 wt.% (Zn), respectively.

Table 2. The wt.% distribution of iron and zinc or nickel in the powders depending on the period of the steel surface contacting with distilled water

***t*, h**	***T*, °C**	**Fe**	**Zn**	**Fe**	**Ni**
		$ZnCl_2$		**$NiCl_2$**	
0	20	94.2	5.8	88.4	11.6
1		82.8	17.2	93.9	6.1
3		81.3	18.7	94.6	5.3
1	50	79.4	20.6	92.4	7.6
		$ZnSO_4$		**$NiSO_4$**	
1	20	69.3	30.7	82.0	18.0
1	50	77.5	22.5	85.9	14.1
		$Zn(NO_3)_2$		**$Ni(NO_3)_2$**	
0	20	79.8	20.2	95.9	4.1
3		82.0	18.0	94.3	6.7
1	50	78.4	21.6	92.1	7.9

The weight ratio Fe : Ni in chloride and nitrate-containing solutions lies in the narrow range 88–96 wt.% for iron and 12–4 wt.% for nickel. But the relatively high concentrations of both zinc 22 (30) wt.% and nickel 14 (18) wt.% are fixed in sulfate-bearing systems. Thus the proportion of Zn and Ni in the powders obtained at 20 °C is higher in the comparison with powders formed at 50 °C.

Thermogravimetric and differential thermal properties of the powders

We have chosen four samples to study the thermal behaviour of the mineral powders formed on the steel surface in the presence of nickel and zinc-containing aqueous salt solutions (Figure 4). The in-depth analysis of nickel-bearing systems permitted us to determine the influence of anion composition on the phase transformation of the powder compounds. In addition, $ZnSO_4$ system was analyzed on account of the presence of mixed Zn(II)-Fe(II-III)-SO_4^{2-} LDH in the phase composition of the corresponding powder.

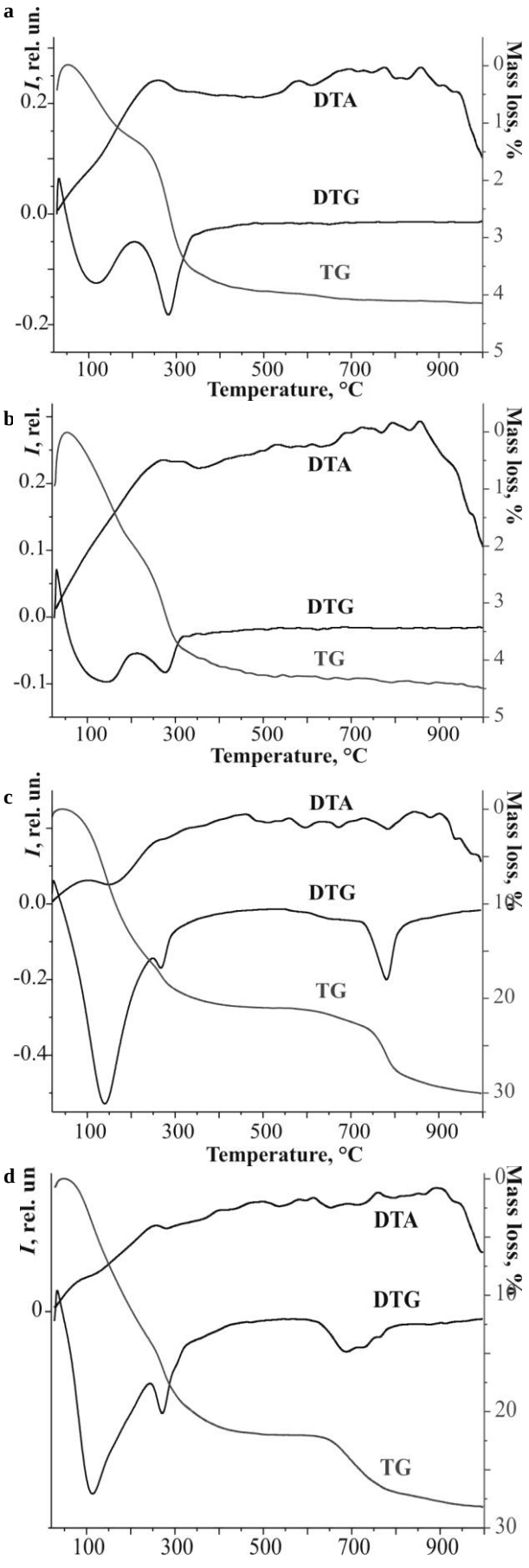

Figure 4. TG-DTA curves of the powders formed on the steel surface in contact with aqueous solutions: a – $NiCl_2$; b – $Ni(NO_3)_2$; c – $NiSO_4$; d – $ZnSO_4$.

According to the experimental data two endo effects are seen in all DTG curves. The first minimum is fixed in the temperature range of 110–137 °C. It corresponds to the loss of the adsorbed water. The second endothermic peak in the temperature range of 270–281 °C is related to the hydroxylation of oxyhydroxide lattice and formation of iron oxide phases. But both sulfate-containing samples show an additional endothermic peak in the temperature range of 622–784 °C ($NiSO_4$) and 725–822 °C ($ZnSO_4$). Those thermal effects are accompanied by the mass loss of the powders on the TG curves (28–30 %) probably because of the phase transformation (dehydroxilation) of mixed LDH and total destruction of SO_4^{2-} species. On the contrary, the mass loss of the nitrate- and chloride-containing samples amounts to 4.5 % only. Two exothermic peaks point to the oxidation of ferrous cations in the spinel ferrite lattice and phase transformation of Fe_3O_4 doped with Ni^{2+} or Zn^{2+} into maghemite γ-Fe_2O_3 at 200–245 °C and polymorphic transformation of γ-Fe_2O_3 into hematite α-Fe_2O_3 at 300–338 °C.

Morphology of the raw and heated powders

The SEM images of the mineral phases formed on the steel surface in contact with aqueous solution of $NiCl_2$ and $Ni(NO_3)_2$ are presented in Figure 5.

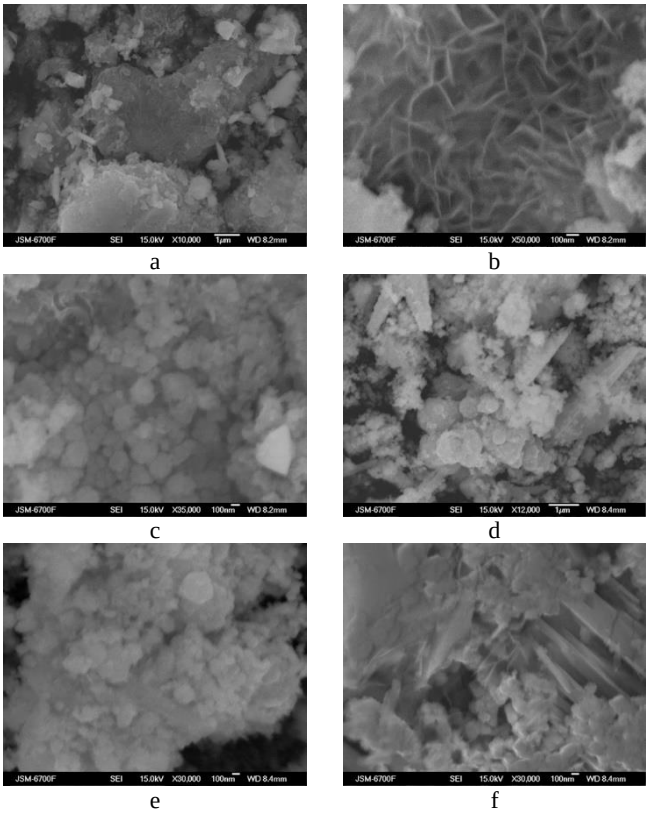

Figure 5. SEM-images of the surface structures formed on the steel surface in contact with aqueous solution of $NiCl_2$: a – the general view, b – mixed Ni(II)-Fe(II-III) LDH, c – spinel ferrite, and $Ni(NO_3)_2$: d – the general view, e – spinel ferrite; f lepidocrocite plates and spherical spinel ferrite particles

Generally, the morphology of the iron-oxygen surface structures is similar and it does not depend on the anion composition of the dispersion medium contacting with the steel surface. Whereas ferric oxyhydroxides are characterized by plate-like or lamellar shape of the particles (Figure 5 a, d, f), the spinel ferrites form spherical particles and aggregates (Figure 5 c, e). The relicts of the mixed Ni(II)-Fe(II-III) LDHs belonging to Green Rust I structure are seen in figure 5 b. Their morphology can be described as chaotic disordered plates and lamellas.

The EDS spectra of the mineral phases formed when the steel surface was in contact with $NiCl_2$ solution show that the average quantity of nickel associated with lepidocrocite phase is ~4.9 wt.%, its quantity in goethite is ~0.75 wt.%, and in spinel ferrite ~ 8.7 wt.%. The manganese and sulfur admixtures got into mineral phases, probably, from the material of the steel. The average content of Fe in all probes reaches ~72.78 wt.%, and content of oxygen equals ~22.23 wt.%.

Magnetic properties of the raw and heated powders

The magnetic study shows that all samples obtained in the presence of the zinc and nickel salt solution have not displayed the residual magnetization (M_r) and coercitivity (H_c). The saturation magnetization (M_s) of the nickel-bearing sample, formed on the steel surface at T = 50 °C within 24 h, equalled 55 $A \cdot m^2 \cdot kg^{-1}$ (Figure 6a). It is interested to note that the increase in temperature has led to reduction of the saturation magnetization of the powders formed in the presence of nickel chloride solutions to 40 $A \cdot m^2 \cdot kg^{-1}$ at 450 °C, and to 7 $A \cdot m^2 \cdot kg^{-1}$ at 750 °C. A powder formed in the presence of nickel sulphate solution showed M_s 32 $A \cdot m^2 \cdot kg^{-1}$ at 450 °C. When zinc chloride solution was used as the dispersion medium the samples formed on the steel surface at T = 50 °C displayed the saturation magnetization 40 $A \cdot m^2 \cdot kg^{-1}$ (Figure 6b). The increase in temperature to 450 °C caused the lowering of parameter M_s up to 5 $A \cdot m^2 \cdot kg^{-1}$ and a further increase of temperature to 750 °C resulted in the increase of M_s to 27 $A \cdot m^2 \cdot kg^{-1}$. Probably, such phenomenon is related to the phase transformation of magnetite into iron oxides doped with zinc cations. Also, the powders obtained at 50 °C in the zinc chloride and nickel sulfate and chloride system demonstrate superparamagnetic properties and, generally, they belong to highly permeable magnetic materials.

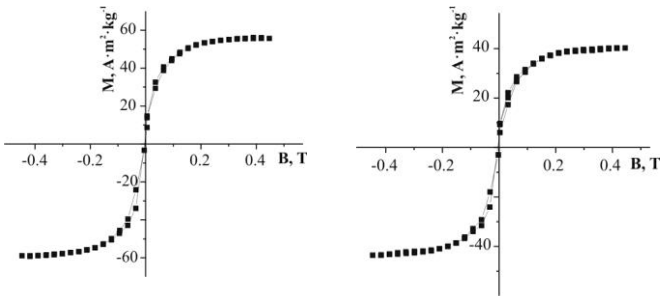

a b

Figure 6. The magnetization curves of the iron-oxygen powders obtained at T = 50 °C on the steel surface when it was contacting with the solutions: a – $NiCl_2$, b – $ZnCl_2$.

Discussion

Depending on the geometrical shape of anions two types of Fe(II)-Fe(III) layered double hydroxides (Green Rusts) may be formed on the steel or iron surfaces. Planar and spherical anions (Cl^-, CO_3^{2-}) coordinate iron hydroxide layers as GR I and three dimension anions (SO_4^{2-}) take place in GR II structure.[16] According to literature data nickel as well as zinc can incorporate into a Green Rust lattice and form various LDH structures corresponding to the first [17, 18] and the second[19-21] lattice's type of Green Rust, respectively. Whereas Fe(II)-Fe(III) LDH under standard conditions do not keep stability against oxidation and solid state transformation into lepidocrocite[22] or its dissolution-re-precipitation into magnetite[23], the mixed LDH structures, due to Fe(II) exchange, lose the possibility for oxidation and, as a result, for phase transformation.

Hence, one of the mixed LDH applications is their thermal treatment to obtain chemically pure mixed oxides at T ~ 450–600 °C[24] or spinel ferrites in the T range from ~ 750 °C[25] to 1100 °C.[26] The formation of pure nickel spinel ferrites via calcination of tailored hydrotalcite-like hydroxysulfate LDH as a single molecular precursor has been mentioned.[27] In such case the precursor species was heated at 900 °C for 2 h to obtain the powder including two phases: α-Fe_2O_3 and NiO, afterwards the oxide mixture was sintered at 1100 °C for 10 h and then slowly cooled to the room temperature. This kind of the procedure is sensitive to metal molar ratios and certain stoichiometry has to be kept. But when the molar ratio of Me^{2+}/Fe^{3+} is broken the non-stoichiometric iron oxides or magnetite doped by 3*d*-metal cations are formed in the system.[28]

The investigation[29,30] of the products of thermal transformation of nickel-containing goethite gives the reason to think that ferric iron is substituted for nickel in the hematite structure. Thus the lattice parameters of hematite formed in the temperature range from 300 to 800 °C are determined by the composition of the precursor phase (ferrihydrite or goethite) containing nickel cations.[31] Moreover, the transformation of nickel-containing goethite into nickel-containing hematite on heating passes through the formation of an intermediate phase of nickel-containing maghemite. In such samples nickel diffuses to the hematite surface within the transformation row Fe_3O_4 – γ-Fe_2O_3 – α-Fe_2O_3[32]. However, in another work[32] it was shown that the heating of maghemite to T < 320 °C leads to the removal of more than 60 % of Co, Ni, Zn, and Cu cations from γ-Fe_2O_3 structure without their subsequent inclusion into hematite structure. But when the hematite obtained by heating maghemite at T = 650 °C for 3 h, it includes small amount of Co, Ni, Zn, Cu, Mn, V, Al, and Cr cations, however, the intensity of its X-ray diffraction peaks does not change.[33] It is possible that the presence of transition 3*d*-metal cations in the structure of maghemite increases the period of its transformation into hematite. This phenomenon has been explained[33] assuming that Co, Ni, Zn, and Cu cations give stability to a cubic lattice of maghemite and complicate its conversion into a hexagonal hematite lattice because some cations are not compatible with hematite structure.

In addition, the role of cations of the dispersion medium in the formation of polymorphic ferric oxyhydroxides has been widely discussed in the literature. The chemical studies[34-36] point out that small amounts of transition metals including Ni, Co, Cr, Mn, Cu, Zn, Cd, and Pb are usually associated with natural and synthetic goethite, whereas such metals as well as Al, Ti, and Mo may also be present in the structure of natural goethite, and hematite.[37,38] The mechanism of cation inclusion into the crystal lattice of goethite is determined via ferric iron substitution and ferric cations may be substituted in goethite lattice for cobalt[39] or nickel[40] cations.

In conformity with our observations, nickel may be included into a goethite lattice without destruction of its crystal structure.[41] Thus, zinc cations protect the lepidocrocite particles against dissolution in ferrous sulfate medium, but nickel ions do not affect the morphology and crystallinity of γ-FeOOH.[42] Ferrous cations are usually adsorbed on the lepidocrocite surface in aqeous medium and may be exchanged for nickel cations to form surface-modified iron oxides.[43] The analysis of our systems confirmed that only γ-FeOOH appeared on the steel surface in contact with all zinc-containing aqeous solutions, but both γ-FeOOH and α-FeOOH co-existed in the phase composition of the powders when the steel surface was in contact with nickel-containing solutions. Hence, the relative quantity of the goethite part was less in comparison with the lepidocrocite part.

The comparison of the powders formed on the steel surface in contact with aqueous solution of zinc and nickel salts with the products of the thermal transformation of mixed LDH precursors formed via co-precipitation of respective salts shows a few differences. Namely, the appearance of the spinel ferrites as a single phase on the steel surface is fixed in the systems where the mixed LDH structures are not formed, for example $Ni(NO_3)_2$ or $Zn(NO_3)_2$ (Figure 3). But when the relatively stable phase of mixed hydroxysulfate LDHs is formed the spinel ferrite is not obtained at T = 20 °C or it co-exists with LDHs and ferric oxyhydroxides at T = 50 °C (Figure 2). In our previous work[13] we have shown that the heating of the copper and cobalt-bearing powders formed under the RCD conditions at T = 740 °C led to the formation of a single hematite phase. No other oxide peaks were present in the XRD patterns. The XRFS study confirmed the association of iron and copper or cobalt cations in the chemical composition of the powders. Moreover, the relative quantity of the doped metal remained the same in the wide temperature range (50–740 °C). So, such powders may be used to obtain monomineralic polymorphic ferric oxides (γ-Fe_2O_3 and α-Fe_2O_3) doped by 3*d*-metal cations.

Conclusions

1. The usage of chloride solutions leads to obtaining of non-stoichiometric spinel ferrites and ferric oxyhydroxides, nitrate salts permit to form the single spinel ferrite phase. But the mixed LDHs appear among powder components in the presence of sulfate solution.

2. TG-DTA analysis of the powders shows four thermal effects corresponding to the loss of the adsorbed water (110–137 °C), hydroxylation (270–281 °C), transformation of Fe_3O_4 doped by Ni^{2+} or Zn^{2+} into maghemite γ-Fe_2O_3 (200–245 °C), and polymorphic transformation of γ-Fe_2O_3

into hematite α-Fe_2O_3 (300–338 °C). But both sulfate-containing samples show an additional endothermic peak accompanied by the mass loss (28–30 %) in the *T* range of 622–822 °C.

3. All mineral phases belong to nano objects and their primary particle size is 10–23 nm for lepidocrocite, 14–23 nm for goethite and ~15–28 nm for spinel ferrite. Depending on the chemical compositions of the water salt solutions the wt.% distribution of the metals in the powders (Fe : Me) varies from 96 : 4 to ~70 : 30.

4. The ferric oxyhydroxides and mixed Ni(II)-Fe(II-III) LDHs have a plate-like or lamellar morphology, and spinel ferrites form spherical particles.

5. All samples obtained in the presence of the zinc and nickel salt solution belong to superparamagnetics and they have not displayed the residual magnetization and coercitivity.

Acknowledgments

We gratefully acknowledge leading research scientist O.A. Vyshnevskyi of Mass-spectrometric centre of solid phase, for gas isotopic trace element analysis. We are thankful to M. P. Semenenko, Institute of Geochemistry, Mineralogy and Ore Formation of NAS of Ukraine, for the obtaining of the SEM images and EDS data. We acknowledge the support from leading research scientist M. V. Borisenko from O. O. Chuiko Institute of Surface Chemistry of NAS of Ukraine for the obtaining of TG-DTA data.

This paper has been presented at the 4th International Conference “Nanotechnologies”, October 24 – 27, 2016, Tbilisi, Georgia (Nano – 2016).

References

[1]Teja, A. S., Koh P.-Y., *Prog. Cryst. Growth Charact. Mater.*, **2009**, *55(1-2)*, 22.

[2]Levy, M., Wilhelm, C., Siaugue, J. M., Horner, O., Bacri, J. C., Gazeau, F., *J. Phys.: Condens. Matter*, **2008**, *20(20)*, 204133.

[3]Pankhurst, Q. A., Connolly, J., Jones, S. K., Dobson, J., *J. Phys. D: Appl. Phys.*, **2003**, *36*, R167.

[4]Chirita, M., Grozescu, I., *Chem. Bull. "Politehnica" Univ. (Timisoara)*, **2009**, *54(68)*, 1.

[5]Kang, Y. S., Risbud, S., Rabolt, J. F., Stroeve, P., *Chem. Mater.*, **1996**, *8(9)*, 2209.

[6]Zhao, N., Ma, W., Cui, Zh., Song, W., Xu, Ch., Gao, M.., *ASC Amer. Chem. Soc. NANO*, **2009,** *3(7)*, 1775.

[7]Fysh, S. A., Clark, P. E., *Phys. Chem. Miner.*, **1982,** *8*, 257.

[8]Shirane, G., Pickart, S. J., Nathans, R., Ishikawa, Y., *J. Phys. Chem. Solids*, **1959**, *10*, 35.

[9]Lei, Y., Cant, N. W., Trimm, D. L., *Catal. Lett.*, **2005**, *103*, 133.

[10]Suber, L., Imperatori, P., Ausanio, G., Fabbri, F., Hofmeister, H., *J. Phys. Chem.*, **2005**, *B 109(15)*, 7103.

[11]Hendy, S. C., Laycock, N. J., Ryan, M.P., *J. Electrochem. Soc.*, **2005**, *152*, B271.

[12]Laurent, S., Forge, D., Port, M., Roch, A., Robic, C., Vander Elst, L., Muller R. N., *Chem. Rev.*, **2008**, *108*, 2064.

[13]Lavrynenko, O. M., Dudchenko, N. O., Pavlenko, O. Yu., Brik, A. B., *Proc. Int. Conf.: NAP*-**2015**, *01001*.

[14]Lavrynenko, O. M., Pavlenko, O. Yu., Shchukin, Yu. S., *Nanoscale Res. Lett.*, **2016**, *11(67)*, 2

[15]Lavrynenko, O. M., Korol, Ya. D., Netreba, S. V., Prokopenko, V. A., *Chem. Phys. Tech. Surf.*, **2010**, *1(3)*, 338.

[16]Génin, J.-M. R, Ruby, C., *Solid State Sci.*, **2004**, *6*, 705

[17]Parida, K. M., Mohapatra, L., *Chem. Eng. J.*. **2012**, *179*, 131.

[18]Refait, Ph., Génin, J.-M. R., *Clay Miner.*, **1997**, *32*, 597.

[19]Ahmed, I. A. M., Shaw, S., Benning L. G., *Miner. Mag.*, **2008**, *72(1)*, 159.

[20]Garófalo Chaves, L. H, Curry, J. E, Stone, D. A, Carducci, M. D., Chorover, J., *Rev. Bras. Cienc. Solo*, **2009**, *33(5)*, 1115.

[21]Refait, Ph., Abdelmoula, M., Simon. L., Génin, J.-M. R., *J. Phys. Chem. Solids*, **2005**, *66*, 911.

[22]Schwertmann, U., Fechter, H., *Clay Miner.*, **1994**, *29*, 8.

[23]Sumoondur, A, Shaw, S., Ahmed, I., Benning, L. G., *Mineral. Mag.*, **2008**, *72(1)*, 201.

[24]Vaccari, A., *Catal. Today*, **1998**, *41*, 53.

[25]Fernández, J. M., Ulibarri, M. A., Labajos, F. M., Rives, V., *J. Mater. Chem.*, **1998**, *8*, 2507.

[26]Liu, J., Li, F., Evans, D. G., Duan, X., *Chem. Commun.*, **2003**, *21(4)*, 542.

[27]Li, F., Liu, J., Evans, D. G., Duan, X., *Chem. Mater.*, **2004**, *16*, 1597.

[28]Ishikawa, T., Nakazaki, H., Yasukawa, A., Kandori, K., Seto, M., *Mater. Res. Bull.*, **1998**, *33(11)*, 1609.

[29]Gerth, J., *Geochim. Cosmochim. Acta*, **1990**, *54(2)*, 363.

[30]Ruan, H. D., Gilkes, R. J., *Clay Miner.*, **1995**, *30*, 55.

[31]Lim-Nunez, R., *MSc Thesis*., Univ. of Western Australia, **1985**.

[32]Sidhu, P. S., Gilkes, R. J., Posner, A. M., *Soil Sci. Soc. Amer. J.*, **1980**, *44*, 135.

[33]Sidhu, P. S., *Clays Clay Miner.*, **1988**, *36(1)*, 31.

[34]Trolard, F., Bourrie, G., Jeanroy, E., Herbillon, A. J., Martin, H., *Geochim. Cosmochim. Acta*, **1995**, *59(7)*, 1285.

[35]Manceau, A., Schlegel, M. L., Musso, M., Sole, V. A., Gauthier, C., Petit, P. E., Trolard, F., *Geochim. Cosmochim. Acta*, **2000**, *64(21)*, 3643.

[36]Carvalho-de-Silva, M. L., Ramos, A. Y., Tolentino, H. C. N., Enweiler, J., Netto, S. M., Alves, M. C. M., *Am. Mineral.*, **2003**, *88*, 876.

[37]Wells, M. A., Fitzpatrick, R. W., Gilkes, R. J., *Clays Clay Miner.*, **2006**, *54(2)*, 176.

[38]Singh, B., Gilkes, R. J., *J. Soil Sci.*, **1992**, *43*, 77.

[39]Gasser, U. G., Jeanray, E., Mustin, C., Barres, O., Nuesch, R., Berthelin, J., Herbillon, A. J., *Clay Miner.*, **1996**, *31*, 465.

[40]Gerth, J., *Geochim. Cosmochim. Acta*, **1990**, *54(2)*, 363.

[41]Inouye, K., Ichimura, K., Kaneko, K., Ishikawa, T., *Corros. Sci.*, **1976**, *6*, 507.

[42]Ishikawa, T., Nagashima, A., Kandori, K., *J. Mater. Sci.*, **1991**, *26*, 6231.

[43]Taylor, R. M., McKenzie, R. M., *Clays Clay Miner.*, **1980**, *28*, 179.

Received: 22.12.2016.
Accepted: 04.02.2017.